1-2021

Hygrothermal Ageing Behavior and Mechanism of Carbon Nanofibers Modified Flax Fiber-Reinforced Epoxy Laminates

Yanlei Wang
Dalian University of Technology

Wanxin Zhu
Dalian University of Technology

Baolin Wan
Marquette University, baolin.wan@marquette.edu

Ziping Meng
Dalian University of Technology

Baoguo Han
Dalian University of Technology

Composites Part A : Applied Science and Manufacturing, Vol. 140 (January 2021): 106142. DOI.

Hygrothermal Ageing Behavior and Mechanism of Carbon Nanofibers Modified Flax Fiber-Reinforced Epoxy Laminates

Yanlei Wang
State Key Laboratory of Coastal and Offshore Engineering, School of Civil Engineering, Dalian University of Technology, Dalian 116024, China
Wanxin Zhu
State Key Laboratory of Coastal and Offshore Engineering, School of Civil Engineering, Dalian University of Technology, Dalian 116024, China
Baolin Wan
Department of Civil, Construction and Environmental Engineering, Marquette University, Milwaukee, WI
Ziping Meng
State Key Laboratory of Coastal and Offshore Engineering, School of Civil Engineering, Dalian University of Technology, Dalian 116024, China
Baoguo Han

State Key Laboratory of Coastal and Offshore Engineering, School of Civil Engineering, Dalian University of Technology, Dalian 116024, China

Abstract

This study investigated the effects of carbon nanofibers (CNFs) content on hygrothermal ageing behaviors and mechanisms of flax fiber-reinforced epoxy (FFRE) laminates. CNFs/FFRE laminates containing 0.25–2.0 wt% CNFs were fabricated and immersed in distilled water for 180 days. Water absorption and tensile as well as thermodynamic properties were investigated. The research results showed that CNFs played a significant role in the improvement of hygrothermal properties of FFRE laminates. The water uptake of CNFs/FFRE laminates was significantly decreased because CNFs improved water barrier properties of the laminates. The improvements of tensile and thermodynamic properties of CNFs/FFRE laminates were attributed to the fact that CNFs strengthened the interface bonding and enhanced the matrix's stability. This study demonstrates that adding appropriate amount of CNFs into FFRE laminates is beneficial to improving the hygrothermal durability of FFRE laminates.

Keywords

A. Carbon nanofibers, A. Natural fibers, A. Nanocomposites, B. Environmental degradation

1. Introduction

In the past few decades, fiber-reinforced polymer (FRP) composites have been widely used in many fields such as automobile, aerospace and construction due to their outstanding mechanical properties, light weight, high strength, corrosion resistance and durability [1], [2], [3], [4], [5], [6], [7], [8], [9], [10]. However, with the consumption of non-renewable resources and the aggravation of severe environmental pollution, it is urgent to find renewable and environmentally friendly fibers to replace the traditional synthetic fibers such as carbon, glass, and basalt fibers. Plant fiber as one kind of renewable fibers is attracting much attention in many fields due to its low density, renewability, and biodegradability as well as cost-effectiveness [11]. Many types of plant fiber (e.g., flax, hemp, sisal, and ramie fiber) reinforced polymers (PFRP) composites have been explored by some researchers [11], [12], [13], [14], [15]. Among the plant fibers which have been studied, flax fiber possesses excellent mechanical properties (400–2000 MPa of tensile strength, 12–85 GPa of tensile modulus, and 1–4% of ultimate strain [16], [17], [18]), which are close to those of glass fiber. Therefore, flax fiber is one of the strongest plant fiber candidates in the pursuit of replacing synthetic fibers [17], [18], [19], [20], [21].

Although flax fiber has excellent mechanical properties, its applications as a load-bearing structural material in civil engineering are limited due to its severe deterioration under hygrothermal conditions. Flax fiber is composed of a primary outer wall and a secondary wall with three different layers, which are mainly made of cellulose, hemicellulose and pectin, and a central hollow region [15], [18], [20]. The cellulose, hemicellulose and pectin contain lots of hydrophilic groups (e.g., hydroxyl), which can attract large number of water molecules. Additionally, the central hollow region of flax fiber is easy to store water. Some studies [15], [18], [20] showed that water immersion would cause degradation of flax fiber and reduce its mechanical properties. In addition, the degradation process of flax fiber would be accelerated under the coupling of water immersion and high temperature due to the poor thermostability of hemicellulose and pectin of flax fiber [21], [22], [23].

For improving the shortcomings of flax fiber, many methods of fiber surface treatment have been explored by researchers [21], [24], [25], [26] to improve its hygrothermal ageing behavior. These methods can be categorized as physical methods (e.g., steam explosion treatment and heat treatment), chemical methods (e.g., alkali treatment), and biological treatment methods (e.g., enzyme treatment). The methods of fiber surface treatment could improve the hygrothermal ageing behavior of flax FRP (FFRP) laminates in their early stage of hygrothermal ageing, but the improvement is not obvious in the long-term hygrothermal ageing [13], [26]. This phenomenon can be explained by two main reasons. First, the polymer matrix begins to be deteriorated, leading to micro-cracks development and voids formation in the matrix, after the FFRP laminates are immersed in water. The deterioration of the polymer matrix will significantly affect the hygrothermal ageing behavior of FFRP laminates. Second, when water enters into the interior of the FFRP laminates through the cracks and the voids of the matrix to corrode the fiber, water will gradually fill the whole lumen of the fiber with the increase of immersion time, causing the benefits of fiber surface treatments to improve hygrothermal ageing behavior is not obvious under the coupling of long-term solution immersion and high temperature [27]. Therefore, in the case where the effect of fiber surface treatment on its hygrothermal ageing behavior is limited, modifying the properties of the polymer matrix might be an alternative method suitable for improving the hygrothermal ageing behavior of FFRP laminates.

Among all methods of modifying the properties of the polymer matrix, adding nanoparticles into the polymer matrix (also called polymer-matrix nanocomposites) is one of the effective methods. Polymer matrix nanocomposites are hybrid materials consisting of nanoparticles dispersed in an organic polymer matrix [28], [29], [30], [31], [32]. Polymer matrix incorporating nanoparticles (i.e., carbon nanotubes (CNTs), Nano-SiO_2, and Nano-clay) have been reported by numerous studies [28], [29], [30], [31], [32], which indicated that the properties of the polymer-matrix nanocomposites after adding nanoparticles were significantly improved. Compared with CNTs, carbon nanofibers (CNFs) have gotten much more attention in last two decades due to their excellent mechanical properties, easy-to-disperse and low manufacturing cost [33], [34], [35]. Some researchers [36], [37], [38] have proven that the incorporation of CNFs in polymer matrix made a greatly enhancement on mechanical, thermal and electrical properties of the matrix. In particular, adding CNFs into the polymer matrix could also improve its hygrothermal resistance [36]. Hence, it will be a feasible method to improve the hygrothermal ageing behavior of FFRP laminates by adding CNFs into the polymer matrix of FFRP laminates.

The method of adding CNFs into polymer matrix to improve their hygrothermal ageing behavior was first developed in synthetic fiber-reinforced composites [39], [40]. Jefferson et al. [39] explored the influence of hygrothermal conditions on CNFs/glass FRP (GFRP) laminates and found that adding 1.0 wt% CNFs into the matrix of GFRP laminates significantly reduced both water saturation level and water diffusivity of the GFRP laminates. Microscopy observation indicated that the bridging effect occurred due to the addition of CNFs, which reduced the degradation of the laminates. Kattaguri et al. [40] studied the influence of CNFs' contents on GFRP laminates immersed in seawater after 150 days. It was found that the hygrothermal durability of 1.0 wt% CNFs/GFRP laminates was more superior to that of 0.1 wt% CNFs/GFRP laminates. However, there is no research to study the hygrothermal ageing behavior of FFRP laminates modified by CNFs. Compared with the traditional fiber surface treatment method (i.e. physical method, and chemical method) [21], [24], [25], [26], using CNFs in the

modification of FFRE laminates to improve their hygrothermal ageing behavior may be expensive. However, as mentioned above, the improvement through traditional fiber surface treatment method is not obvious in the long-term hygrothermal ageing for FFRE laminates [13], [26]. It might be a cost-effective alternative to enhance the long-term hygrothermal ageing behavior of FFRE laminates modified by CNFs. Therefore, it is necessary to comprehensively evaluate the hygrothermal ageing behavior of FFRP laminates modified by CNFs, which will be helpful to expand the application of FFRP laminates in moist environment.

The objectives of this research are to investigate the effect of CNFs on the hygrothermal ageing behavior of flax fiber-reinforced epoxy (FFRE) laminates subjected to distilled water immersion, and to explore the hygrothermal ageing mechanism of FFRE laminates modified by CNFs. In this study, CNFs/FFRE laminates with 0 to 2.0 wt% of CNFs were fabricated by wet lay-up method. All samples were immersed in 20 °C, 40 °C, and 60 °C distilled water for 180 days, respectively, to study the water absorption of CNFs/FFRE laminates. Tensile and thermodynamic properties of the CNFs/FFRE laminates were also investigated at different ageing time. Scanning electron microscope (SEM) and Fourier transform infrared (FTIR) spectrum were conducted to characterize the changes of hygrothermal ageing of the CNFs/FFRE laminates. Moreover, the corresponding hygrothermal ageing mechanism of CNFs/FFRE laminates immersed in distilled water was also explored.

2. Experimental program

2.1. Materials and fabrication

The bi-directional flax fiber fabrics were chosen as the reinforcement of FFRE laminates. The area density and normalized thickness of flax fabrics were 240 g/m^2 and 0.16 mm, respectively. An epoxy resin including main agent and curing agent with a weight ratio of 10:3 was adopted as the matrix of FFRE laminates. CNFs were adopted as nanofillers in the FFRE laminates. The average diameter and length of CNFs were 100 nm and 50–200 μm.

The fabrication procedure of CNFs modified FFRE laminates is schematically shown in Fig. 1 and described in following. (1) Four amounts of CNFs (i.e., 0.25%, 0.5%, 1.0%, and 2.0% by weight of the epoxy resin matrix), which had been dried in an oven before weighing to remove any possible moisture in them, were mixed with acetone by using a high-speed mechanical agitator for 30 min with a rotating speed of 2000 rpm. (2) Sonication for the CNFs/acetone mixture was followed by placing the solution in an ultrasonic cleaner for 6 h at 60 °C to facilitate the dispersion. (3) The CNFs/acetone mixture was added into the epoxy main agent, and then was subjected to mechanical agitation and ultrasonic dispersion to get a CNFs/epoxy mixture with uniform dispersion. The acetone in the mixture was volatilized completely during mechanically stirring. (4) To remove the bubbles in the CNFs/epoxy mixture, the CNFs/epoxy mixture was kept in a vacuum oven for 20 min. (5) The curing agent was added into the CNFs/epoxy mixture with low-speed stirring (a rotating speed of 500 rpm) for 5 min. The mixture was then degassed in the vacuum oven for 20 min. (6) The CNFs/FFRE laminates including two layers of bi-directional flax fiber fabrics with the dimensions of 350 mm × 350 mm were made by the method of wet lay-up. The laying direction of the two flax fiber fabrics were kept same. (7) The CNFs/FFRE laminates were firstly cured at room temperature for 24 h and then placed in an oven set at 60 °C for additional 24 h. The CNFs/FFRE laminates were then kept at room temperature for additional

168 h (7 days) before being immersed in distilled water at different temperatures for ageing and testing. The thickness of the cured CNFs/FFRE laminates was 1.3 ± 0.2 mm. The fiber volume ratio of the laminates is about 0.25. And the weight ratio of epoxy resin to flax fabric in the laminates is about 9:4. In this paper, the FFRE and the CNFs/FFRE laminates containing 0.25 wt%, 0.5 wt%, 1.0 wt%, and 2.0 wt% CNFs were denoted as F_0, $F_{0.25}$, $F_{0.5}$, $F_{1.0}$, and $F_{2.0}$, respectively.

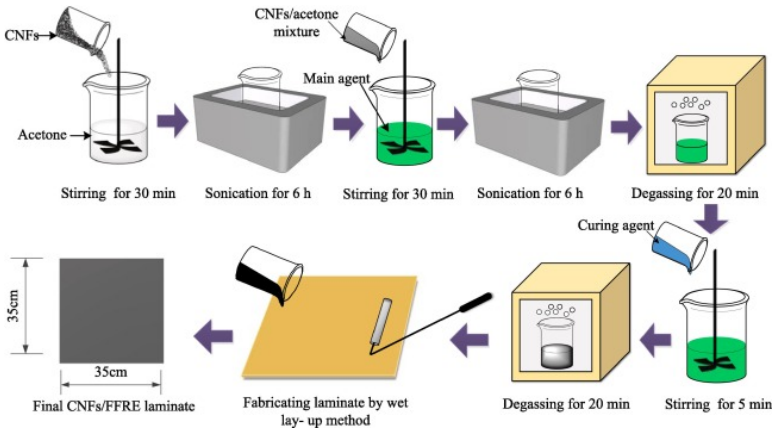

Fig. 1. Schematic procedure to fabricate the CNFs/FFRE laminates. (For interpretation of the references to colour in this figure legend, the reader is referred to the web version of this article.)

The specimens for each type of test in this study were obtained by cutting from the laminates. Four types of test samples (i.e., water absorption test, tensile test, dynamic mechanical analysis (DMA), and FTIR) are shown in Fig. 2.

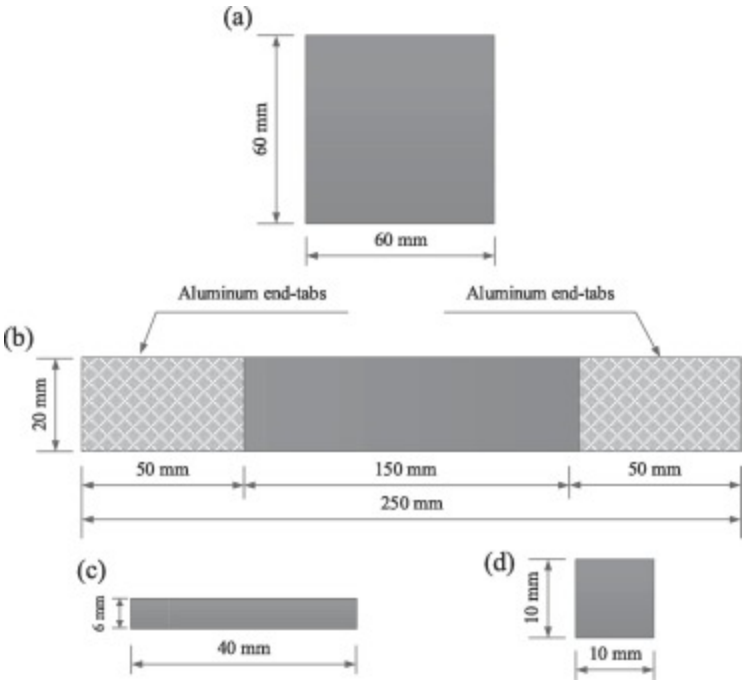

Fig. 2. Test specimens of (a) water absorption test according to ASTM D570 [41]; (b) tensile test according to ASTM D3039 [42]; (c) DMA according to ASTM D4065 [43]; and (d) FTIR.

2.2. Water absorption test

The water absorption test was performed according to ASTM D570 [41]. In order to assess the water absorption of the pure FFRE and CNFs/FFRE laminates, the samples were immersed in distilled water at 23 °C, 40 °C, and 60 °C, respectively, for up to 180 days. The samples were weighed periodically using an electronic balance with a measurement precision of 0.1 mg. At the specific time intervals, which are listed Table 1, the wet samples were taken out from distilled water and wiped with a cloth quickly to remove the surface water before weighing. The water uptake M_t of a sample was calculated by Eq. (1).

$$M_t = \left(\frac{W_t - W_0}{W_0}\right) \times 100\% \quad (1)$$

where W_t is the weight of the wet sample at a specific time interval t, and W_0 is the weight of the dry sample. For each laminate with same amount of CNFs, the average water absorption of ten samples was adopted.

Table 1. Ageing time intervals.

Test type	**Ageing time**
Water absorption	0 h, 1 h, 2 h, 4 h, 8 h, 1 day, 2 days, 4 days, 7 days, 14 days, 30 days, 90 days, 180 days
Tensile properties	0 day, 7 days, 14 days, 30 days, 90 days, 180 days

2.3. Tensile test

The tensile test was carried out according to ASTM D3039 [42] by using a uniaxial tensile testing machine at a loading speed of 2 mm/min. The tensile samples containing different amounts of CNFs were immersed in distilled water at 40 °C for the maximum duration of 180 days. Five samples for each group were tested at the specific time intervals of tensile test listed in Table 1. During the tensile test, an extensometer with a gauge length of 50 mm was attached to the specimen to measure the tensile strain.

2.4. Scanning electron microscopy

The micro-morphologies of the fractured tensile samples before and after ageing were observed by using a SEM instrument. All samples were coated with a gold layer for conductivity before observation. To eliminate the influence of variation, three samples for each group were observed.

2.5. Dynamic mechanical analysis

All dynamic mechanical analysis (DMA) samples were immersed in distilled water at 40 °C for the maximum duration of 90 days, and three samples were tested for each group at specific time intervals. The thermodynamic properties of the FFRE and CNFs/FFRE laminates were characterized by a dynamic mechanical analyzer. The test mode of DMA was in a single cantilever mode at a frequency of 1 Hz. The test temperature was set from room temperature to 140 °C with a heating rate of 2 °C/min. Storage modulus (E'), loss factor ($\tan\delta$), loss modulus (E''), and glass transition temperature (T_g) of the samples were recorded.

2.6. FTIR analysis

The changes of bands and functional groups of FFRE composites after the addition of CNFs were characterized by a FTIR instrument. The CNFs/FFRE laminates exposing to the hygrothermal environment at 40 °C for 90 days were also analyzed by FTIR spectrum. Five samples for each group were prepared, and each sample was scanned at a resolution of 4 cm^{-1} to obtain a spectrum in the wavenumber range 650–4000 cm^{-1}.

3. Results and discussions

3.1. Water absorption

The water uptakes of pure FFRE and CNFs/FFRE laminates for a maximum duration of 180 days are shown in Fig. 3. It can be observed from Fig. 3 that the water uptake of CNFs/FFRE laminates with various amounts of CNFs decreased obviously compared with that of pure FFRE laminates. After 180 days of ageing, the water uptakes of $F_{0.25}$, $F_{0.5}$, $F_{1.0}$ and $F_{2.0}$ decreased by 13.0%, 20.0%, 18.2%, and 16.9% at 23 °C, and 4.3%, 19.4%, 28.1%, and 23.7% at 40 °C, respectively, compared with those of F_0. When the temperature of distilled water was increased to 60 °C, the water uptakes of $F_{0.25}$, $F_{0.5}$, $F_{1.0}$, and $F_{2.0}$ still decreased by 8.5%, 13.6%, 13.6%, and 10.6%, respectively, compared with that of F_0. This means that addition of CNFs in FFRE laminates played a positive role on the decrease of water uptake, even in a high-temperature environment. As the CNFs amount was increased from 0 to 2.0 wt%, the water uptake of CNFs/FFRE laminates declined initially until 1.0 wt% CNFs, and then increased with the increase of the amount of CNFs from 1.0 wt% to 2.0 wt%. The increase of water uptake in the samples with relatively large amount of CNFs (i.e. 2.0 wt%) could be due to the poor dispersion of CNFs in the epoxy matrix in those samples. The dispersion of CNFs with the content of 1.0 wt% and 2.0 wt% in the epoxy matrix can be observed from the SEM images in Fig. 4. Fig. 4a shows that 1.0 wt% CNFs were dispersed uniformly in the epoxy matrix. However, some agglomerations appeared when the content of CNFs was increased to 2.0 wt% as shown in Fig. 4b. These agglomerations of CNFs might cause some defects to weaken the water-resistance of the epoxy matrix. A similar phenomenon was also found in other literature [36].

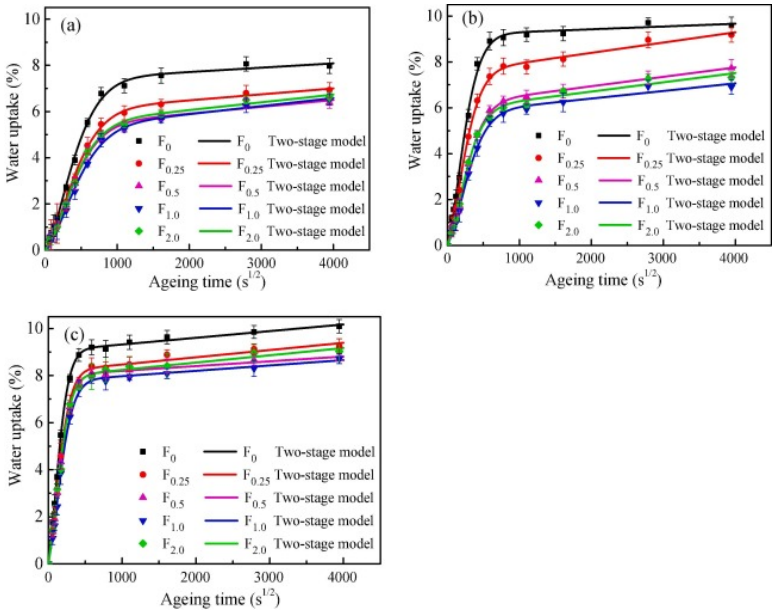

Fig. 3. Water uptake of the FFRE and CNFs/FFRE laminates as a function of the square root of time in distilled water at (a) 23 °C, (b) 40 °C and (c) 60 °C. (For interpretation of the references to colour in this figure legend, the reader is referred to the web version of this article.)

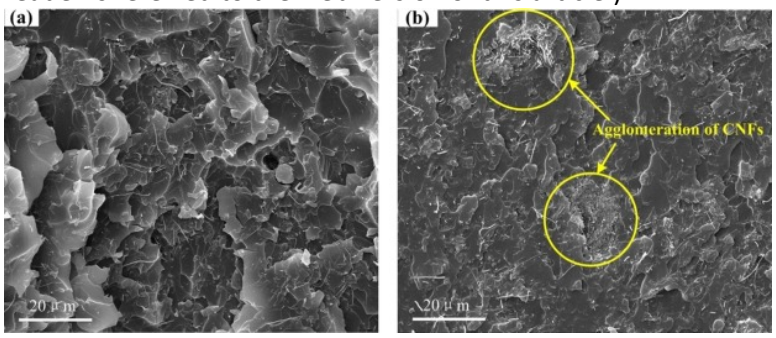

Fig. 4. Dispersion of (a) 1.0 wt%, and (b) 2.0 wt% CNFs in FFRE laminates. (For interpretation of the references to colour in this figure legend, the reader is referred to the web version of this article.)

For pure FFRE and CNFs/FFRE laminates, the changing trends of water uptake showed that the water uptake increased linearly and quickly with the time in the beginning, and then became slower after certain immersion time, which follows the Two-stage model [44]. Eq. (2) can be used to calculate the parameters of the Two-stage model.

$$M(t) = M_{\infty}\left(1 + k\sqrt{t}\right)\left\{1 - \frac{8}{\pi^2}\sum_{j=0}^{\infty}\frac{\exp[-(2j+1)^2\pi^2\left(\frac{Dt}{h^2}\right)}{(2j+1)^2}\right\} \quad (2)$$

where M_∞ is the effective equilibrium water uptake, $M(t)$ is the water uptake at predetermined time intervals t, D is the effective diffusion coefficient, and h is the thickness of the laminates.

As shown in Fig. 3, the fitting curves using Eq. (2) are consistent with the actual test results. The water uptake parameters (i.e., equilibrium water uptake M_∞ and diffusion coefficient D) of the two-stage model for CNFs/FFRE laminates at different temperatures could be determined using Eq. (2). Fig. 5 presents the equilibrium water uptake M_∞ of CNFs/FFRE laminates containing different contents of CNFs in distilled water at 23 °C, 40 °C, and 60 °C, respectively. As shown in Fig. 5, the values of M_∞ of all CNFs/FFRE laminates were smaller than those of pure FFRE laminates at different temperatures. Among these CNFs/FFRE laminates containing different amounts of CNFs, $F_{1.0}$ exhibited the best performance on water resistance. Comparing to F_0, the M_∞ of $F_{1.0}$ decreased apparently by 29.3%, 37.5%, and 14.4%, at 23 °C, 40 °C, and 60 °C, respectively. The values of diffusion coefficient D of CNFs/FFRE laminates containing different content of CNFs in distilled water at 23 °C, 40 °C, and 60 °C are shown in Fig. 6. The diffusion coefficient D is closely related to the slope of the initial linear part of the water uptake curves shown in Fig. 3, and has significantly effect on the ageing time to reach water saturation and the amount of water uptake. It can be seen in Fig. 6 that the values of D decreased at first and then increased with the increase of CNFs, and all of them were lower than those of F_0 at all three temperatures tested in this study. This indicates that the addition of CNFs had an excellent barrier function on water diffusion. The value of D was also highly sensitive to the temperature of the

distilled water. The data showed that the rate of water diffusion inside of samples was accelerated as the temperature was increased. The increase of *D* led to an increase in the equilibrium water uptake M_∞, which can be observed from Fig. 5, Fig. 6.

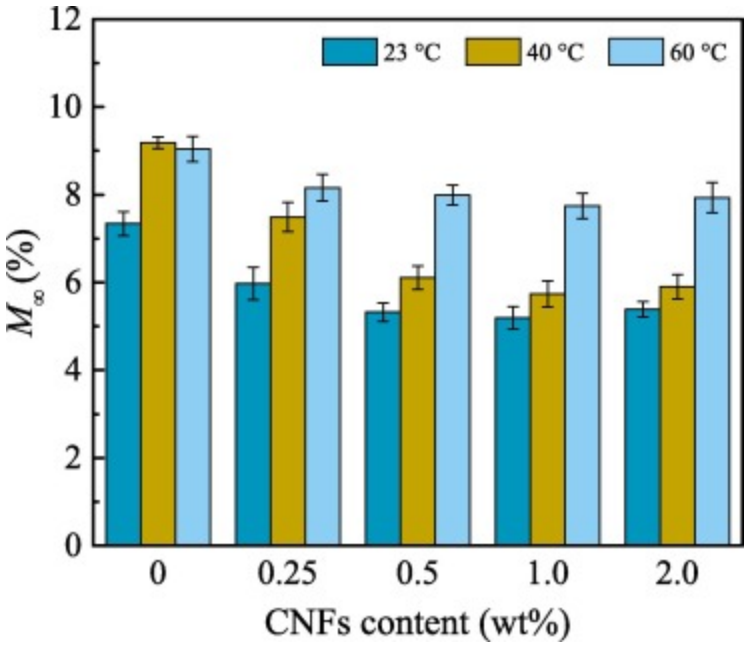

Fig. 5. Equilibrium water uptake M_∞ of CNFs/FFRE laminates containing different contents of CNFs in distilled water at 23 °C, 40 °C, and 60 °C. (For interpretation of the references to colour in this figure legend, the reader is referred to the web version of this article.)

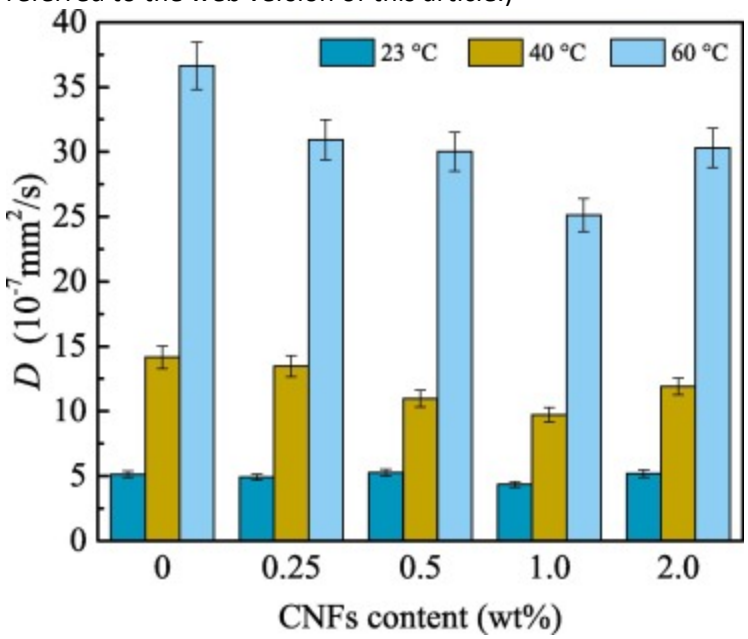

Fig. 6. Diffusion coefficient *D* of CNFs/FFRE laminates containing different contents of CNFs in distilled water at 23 °C, 40 °C, and 60 °C. (For interpretation of the references to colour in this figure legend, the reader is referred to the web version of this article.)

The reduction of water uptake of the CNFs/FFRE laminates after adding CNFs can be explained by two reasons. On one hand, since the hydrophobic of CNFs is in contrast to the hydrophily of flax fiber, CNFs occupy a certain free-volume inside the matrix, and therefore reduce the volume for water molecules.

On the other hand, CNFs as a barrier medium hinders the water diffusion [45] because the water molecules need to go through a tortuous diffusion path in the CNFs/FFRE aminates as shown in Fig. 7.

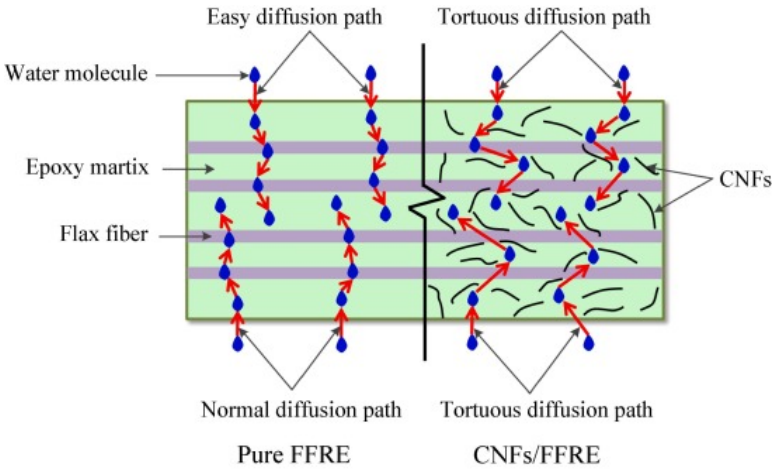

Fig. 7. Different diffusion paths of water in pure FFRE and CNFs/FFRE laminates. (For interpretation of the references to colour in this figure legend, the reader is referred to the web version of this article.)

3.2. Tensile test

The tensile properties (i.e., tensile strength, tensile elastic modulus, and elongation at break) of pure FFRE and CNFs/FFRE laminates with 0.25 wt% to 1.0 wt% CNFs vs. ageing time are presented in Fig. 8. The tensile strengths (Fig. 8a) of all aged samples decreased by 20–25% after 180 days of immersion compared with that of unaged samples. As the CNFs amounts were increased from 0 to 1.0 wt%, the tensile strengths of unaged and aged specimens were improved gradually. For example, the tensile strength of $F_{1.0}$ decreased from 195.0 MPa to 145.8 MPa after the ageing of 180 days, while that of F_0 decreased from 172.0 MPa to 130.9 MPa after the same ageing period. The final tensile strength of $F_{1.0}$ after the ageing of 180 days was still 11.1% higher than that of F_0. It can be found from Fig. 8b that the tensile elastic modulus of the samples was gradually improved with the increase of CNFs content before ageing. After they were immersed in distilled water for 180 days, the tensile elastic modulus of all samples degraded severely. Among these CNFs/FFRE laminates, $F_{0.25}$, $F_{0.5}$, and $F_{1.0}$ decreased from 15.4 GPa to 10.1 GPa, from 15.6 GPa to 10.2 GPa, and from 17.4 GPa to 10.4 GPa, respectively, but all them were higher than those of F_0 (from 13.0 GPa to 9.8 GPa). The CNFs/FFRE laminates containing 1.0 wt% CNFs had highest tensile modulus in all ageing stages among all CNFs/FFRE samples.

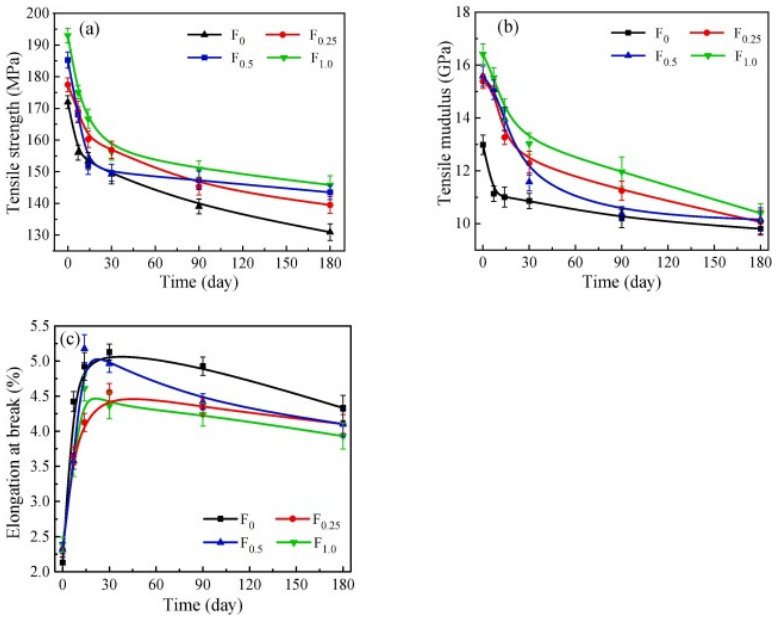

Fig. 8. Effect of hygrothermal ageing on the tensile properties of pure FFRE and CNFs/FFRE laminates. (a) Tensile strength, (b) Tensile elastic modulus, and (c) Elongation at break. (For interpretation of the references to colour in this figure legend, the reader is referred to the web version of this article.)

The changing trend of elongation at break after ageing as shown in Fig. 8c was different from those of tensile strength and tensile elastic modulus. The elongations at break of aged samples within the ageing of 30 days showed substantial improvement compared to those of the unaged samples. This is because the samples became softer after absorbing water. After 30 days of ageing, the elongation at break gradually decreased due to the deterioration and plasticization of polymer matrix and the ageing of flax fibers. It was observed that the elongations at break of CNFs/FFRE laminates were lower than that of pure FFRE laminates after ageing. This might be because the addition of CNFs in FFRE laminates increased the stiffness of the laminates, leading to a decrease of deformability.

Fig. 9 shows the relationship between the tensile properties of pure FFRE and CNFs/FFRE laminates with different amount of CNFs and the water uptake. There was a strong correlation between the tensile strength/modulus of all samples and the water uptake (Fig. 9a and b). The tensile strength and modulus of all samples gradually degraded with the increase of the water uptake. The degradation rate of the tensile strength and modulus increased significantly after the equilibrium water uptake (about at the ageing time of 14 day) was reached. As shown in Fig. 9c, the elongations at break of the samples increased before 30 days of ageing (the third interval of tensile tests), and decreased afterwards with the increase of the water uptake.

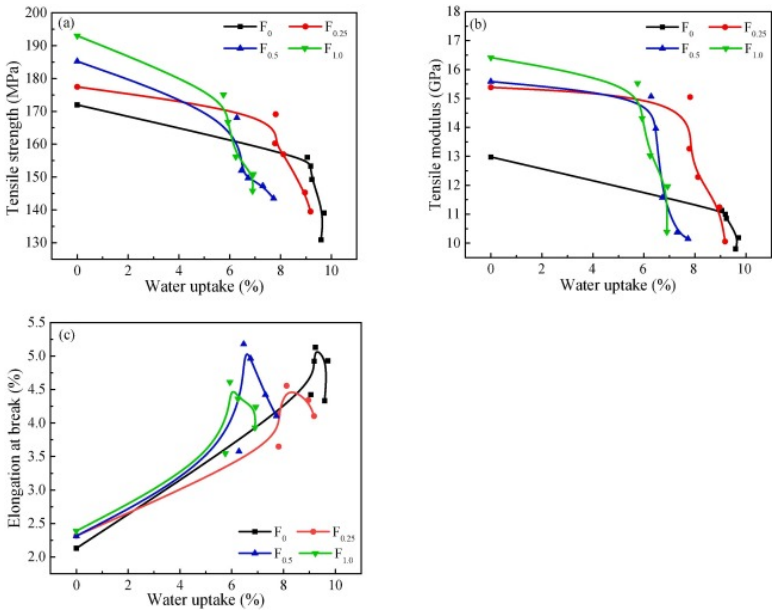

Fig. 9. Tensile properties of pure FFRE and CNFs/FFRE laminates vs. water uptake. (a) tensile strength, (b) tensile elastic modulus, and (c) elongation at break. (For interpretation of the references to colour in this figure legend, the reader is referred to the web version of this article.)

3.3. Morphological characterization

In order to understand the improvement of tensile properties of CNFs/FFRE laminates after ageing, failure analysis was conducted on fractured samples by observing the microscopic morphology. Fig. 10a and b present the sample surfaces of F_0 and $F_{1.0}$ after 90 days of ageing, respectively. It can be found that a lot of cracks and voids developed in the epoxy matrix without CNFs (Fig. 10a), but less damage was in the CNFs/epoxy matrix (Fig. 10b). Fig. 10c and d show the magnified morphologies of pure epoxy matrix and CNFs/epoxy matrix, respectively. Many micro-cracks and voids can be observed in Fig. 10c, which were caused by the swelling and plasticization of epoxy resin. However, there were only a few slight defects (e.g., pittings) that developed in the CNFs/epoxy matrix, as shown in Fig. 10d. This could be explained by that the CNFs with high specific surface area inhibited the movement of the epoxy molecular chains, and therefore improved the stability of the epoxy matrix [46]. Moreover, the formation of micro-cracks in the epoxy matrix might also be caused by the different thermal expansivities between the flax fiber and the epoxy matrix. The presence of CNFs playing as bridging inhibited the generation of micro-cracks in the epoxy matrix [47].

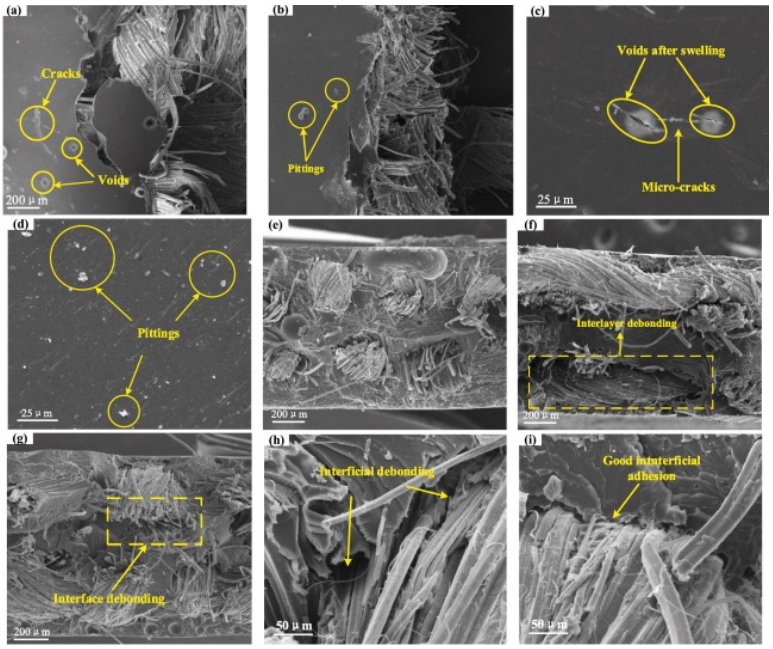

Fig. 10. Sample surfaces of F_0 (a and c) and $F_{1.0}$ (b and d) after 90 ageing days. Fracture surfaces of unaged F_0 (e), 90-days aged F_0 (f) and $F_{1.0}$ (g). Interfacial adhesion of (h) F_0 and (i) $F_{1.0}$ after 90 ageing days. (For interpretation of the references to colour in this figure legend, the reader is referred to the web version of this article.)

The interface status between the epoxy matrix and the flax fibers of pure FFRE laminates before and after ageing can be seen from Fig. 10e and f, respectively. Fig. 10e shows that there was no significant interfacial separation between the epoxy matrix and the flax fibers of unaged pure FFRE laminates, which displayed a good interfacial bonding before ageing. After 90 days of ageing, interfacial damages were developed in the pure FFRE laminates (Fig. 10f). For the 1.0 wt% CNFs/FFRE laminates, the degree of debonding between the epoxy matrix and the flax fibers as shown in Fig. 10g was less severe than that of pure FFRE laminates. The magnified debonding of pure FFRE laminates (Fig. 10h) showed a large area of interface debonding. However, the CNFs/FFRE laminates (Fig. 10i) had better fiber/matrix interfacial bonding. Some studies [48], [49], [50], [51], [52], [53] have shown that the interfacial bonding between the reinforcing fiber and the resin matrix would be increased significantly due to the addition of nano-fillers into the resin matrix. Park et al. [48] measured the interfacial shear strength (IFSS) between the glass fiber and the epoxy resin modified by CNTs through microdroplet pullout tests. Their test results indicated that the IFSS value of the glass fiber/CNT-epoxy nanocomposites increased from 44.9 MPa to 56.9 MPa compared with that of the glass fiber/neat-epoxy composites. Ahmadi et al. [49] investigated the IFSS between ultrahigh molecular weight polyethylene (UHMWPE) fiber and CNFs-epoxy resin via microdroplet pullout tests. It was found that the IFSS value increased from 1.93 MPa to 2.10 MPa in the UHMWPE fiber/CNFs-epoxy nanocomposites with 0.5 wt% CNFs, compared with that of fiber/neat-epoxy composites. The test results of Mohammadalipour et al. [50] also showed that the IFSS value between the UHMWPE fiber and the epoxy resin increased from 2.40 MPa to 5.23 MPa when 3.0 wt% nano-clay was added into the neat epoxy resin. In addition to IFSS, the interlaminar shear strength (ILSS) can also reflect the interfacial bonding between the fiber and the matrix. Through short-beam bending test, Wu et al. [51] found that the ILSS of the carbon fiber/CNTs-methylphenylsilicone resin (MPSR) nanocomposites filled with 0.5 wt% CNTs is 34.14 MPa, which is higher than that of carbon fiber/neat-MPSR composites (30.52 MPa). Shen et al. [52] observed

that the ILSS value between the ramie fiber and CNTs-epoxy with 0.6 wt% CNTs, was 38% higher than that of the counterpart without CNTs. Therefore, the interfacial bonding between the flax fiber and the epoxy resin modified by CNFs in this study is also expected to be increased due to the addition of CNFs into the matrix.

Through analyzing the fracture surfaces of pure FFRE and CNFs/FFRE tensile samples before and after ageing, it can be concluded that the addition of CNFs not only improved the stability of the epoxy matrix, but also strengthened the interface bonding between the epoxy matrix and the flax fibers. Fig. 11a shows that the CNFs were pulled out during the tensile test. This demonstrates that CNFs with excellent mechanical properties could bear the tensile force during the test. In addition, CNFs could be used as a transmission medium that changed the path of tensile force being transferred within the specimen, which reduced the stress concentration. Moreover, the significant bridging effect of CNFs strengthened both the compactness of the matrix itself and the interfacial bonding between the fibers and the matrix as shown in Fig. 11b, 11c, and 11d. Therefore, the long-term tensile properties of CNFs/FFRE laminates were improved compared with that of pure FFRE laminates.

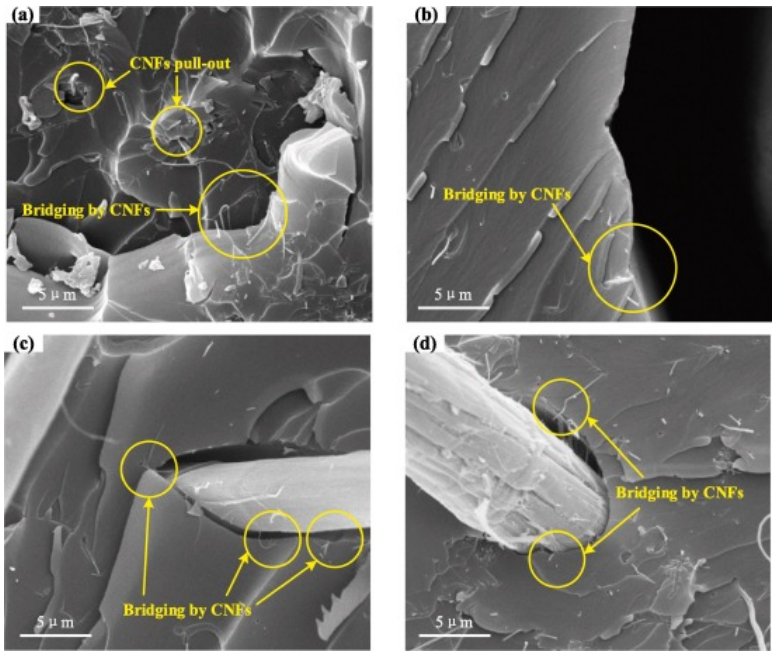

Fig. 11. Bridging of CNFs after tensile failure between (a) and (b) matrix and matrix, (c) and (d) fiber and matrix. (For interpretation of the references to colour in this figure legend, the reader is referred to the web version of this article.)

3.4. DMA

To analyze the viscoelastic properties of FFRE laminates with various amounts of CNFs after hygrothermal ageing, the variation in thermodynamic parameters (i.e., E', E'', and tanδ) are shown in Fig. 12, Fig. 13, Fig. 14. Fig. 12 presents the storage modulus E' of CNFs/FFRE laminates before and after ageing. When 1.0 wt% CNFs were incorporated into FFRE laminates, a maximum improvement of E' was 21.5% compared with that of pure FFRE samples. After immersed in distilled water at 40 °C for 90 days, the storage moduli E' of all samples experienced a considerable reduction as shown in Fig. 12b. For F_0, $F_{0.25}$, and $F_{1.0}$, the E' of 90-days aged samples decreased from 3452.8 MPa to 2750.2 MPa,

3054.9 MPa to 2604.3 MPa and 2463.9 MPa to 2001.3 MPa, respectively. It can be seen that the *E*′ of $F_{1.0}$ remained higher than those of F_0 and $F_{0.25}$, which means that the appropriate amount of CNFs was beneficial for improving the stiffness of FFRE composites. The enhancement of *E*′ after adding CNFs in FFRE laminates can be attributed to that the addition of CNFs made steric hindrance inside the epoxy matrix, which limited the mobility of the molecular chains and decreased the deformation of molecular chains [36]. The thermostability of CNFs/FFRE laminates was better than that of pure FFRE laminates. In addition, the physical aggregation of molecular chains on the surface of CNFs increased the cross-linking density of epoxy resin [39].

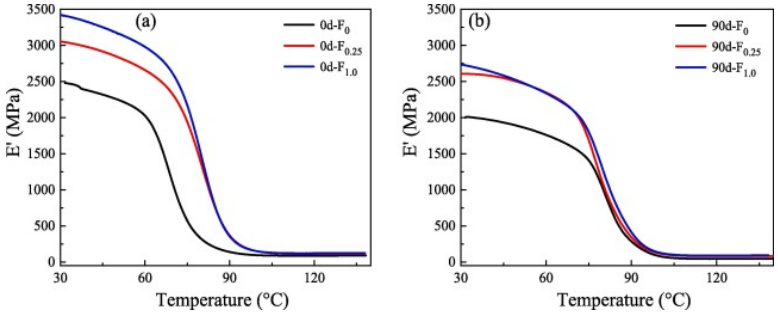

Fig. 12. Variation in storage modulus (*E*′) with temperature for FFRE laminates with various CNFs content after (a) 0 day and (b) 90 days of hygrothermal ageing. (For interpretation of the references to colour in this figure legend, the reader is referred to the web version of this article.)

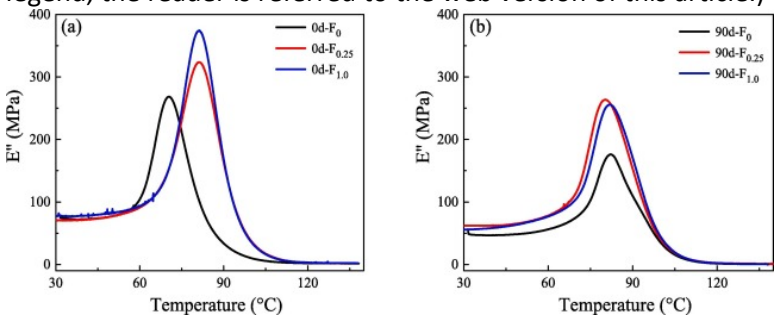

Fig. 13. Variation in loss modulus (*E*″) with temperature for FFRE laminates with varying CNFs content after (a) 0 day and (b) 90 days of hygrothermal ageing. (For interpretation of the references to colour in this figure legend, the reader is referred to the web version of this article.)

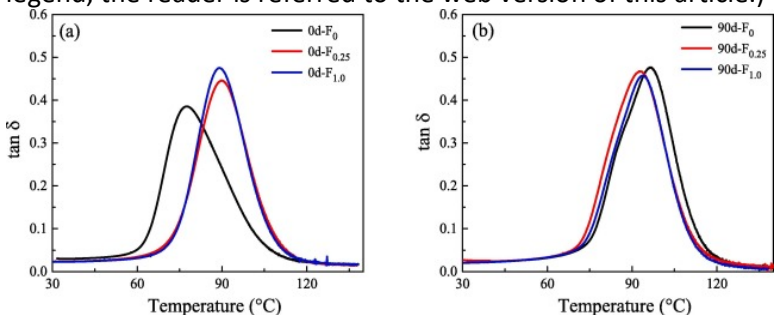

Fig. 14. Variation in loss factors (tan*δ*) with temperature for FFRE laminates with varying CNFs content after (a) 0 day and (b) 90 days of hygrothermal ageing. (For interpretation of the references to colour in this figure legend, the reader is referred to the web version of this article.)

The loss modulus (*E*″) and loss factor (tan*δ*) are important parameters to evaluate the ability to dissipate energy for FRP composites during deformation. The plots of *E*″ vs. temperature of pure FFRE and CNFs/FFRE laminates before and after ageing are displayed in Fig. 13. It can be clearly observed in

Fig. 13 that the peak values of *E*" of CNFs/FFRE laminates were higher than that of pure FFRE laminates no matter ageing or not, which means that CNFs/FFRE laminates dissipated more energy due to the friction between CNFs and epoxy molecules. Fig. 14 shows the variation of *tanδ* vs. temperature for pure FFRE and CNFs/FFRE laminates. It reveals that the peak values of *tanδ* of CNFs/FFRE laminates were higher than that of pure FFRE laminates before ageing. The value of *tanδ* of $F_{1.0}$ was also higher than of $F_{0.25}$, which reflects that the viscosity for shock absorption of 1.0 wt% CNFs/FFRE laminates was better than both pure FFRE and 0.25 wt% CNFs/FFRE laminates before ageing. After ageing for 90 days, both pure FFRE and CNFs/FFRE laminates showed a similar peak as shown in Fig. 14b. This phenomenon could be attributed to that the long-term hygrothermal ageing made a severe degradation of the thermodynamics properties of all samples, which caused the effect of CNFs was not obvious.

Glass transition temperature (T_g) is the highest temperature for FRP composites to be used in practice. Fig. 15 shows the T_g of the pure FFRE and CNFs/FFRE laminates at certain ageing periods. Before ageing, the T_g of FFRE laminates was increased as the CNFs amount was increased. When the amount of CNFs was increased to 1.0 wt%, T_g was increased from 69.7 °C to 76.5 °C. The increase of T_g after adding CNFs can be attributed to that CNFs can limit the deformability of epoxy resin matrix by restricting the mobility of epoxy molecular chains. Additionally, as discussed in the part of *E*', physical aggregation of molecular chains on the surface of CNFs increased the cross-linking density of epoxy resin, which also helps to increase T_g.

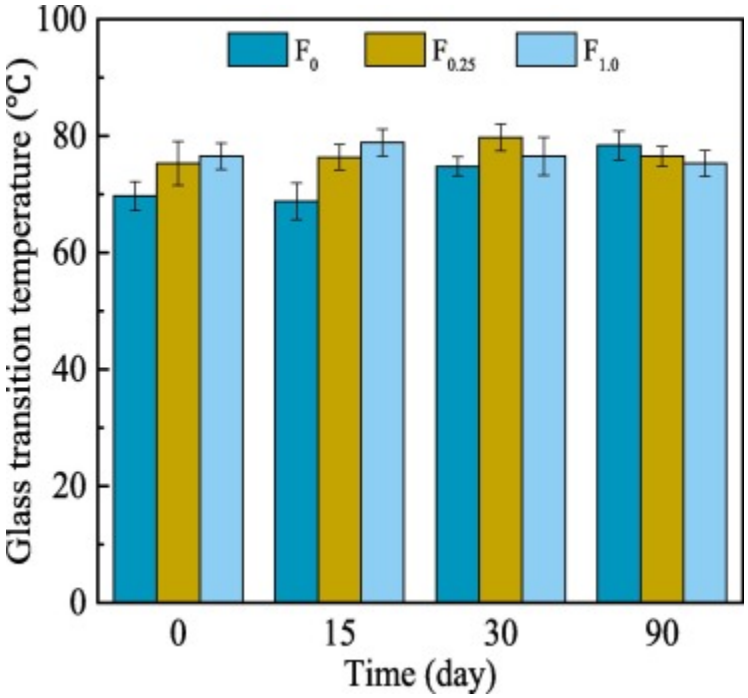

Fig. 15. Variation in glass transition temperature with temperature for FFRE laminates with different content of CNFs after 0 day, 15 days, 30 days, and 90 days hygrothermal ageing. (For interpretation of the references to colour in this figure legend, the reader is referred to the web version of this article.)

It can be noticed that the T_g of all samples tended to be similar and have a slight increase after ageing during a period of immersion time as shown in Fig. 15. This phenomenon was also found in other

studies [46], [53], [54]. As shown in Fig. 16, the types of binding water can be classified into a Type I or Type II bound water according to the activation energy and bond complex between water and epoxy matrix [53]. The bonding of Type I water with low activation is not as strong as the bonding of epoxy structure while the bonding of Type II water with high activation is stronger than that of epoxy structure [46]. At the beginning of the ageing, a large amount of Type I bound water occupied the interior of the epoxy matrix, combining with the epoxy molecular chains to form the single hydrogen bond (Fig. 16a). These single hydrogen bonds are easy to be removed from those epoxy molecular chains. With the increase of immersion time, Type II bound water gradually filled the epoxy matrix, which can form multiple hydrogen bonds combined with the epoxy molecular chains (Fig. 16b). The multiple hydrogen bonds not only are difficult to destroy, but also can form new cross-linking networks of the epoxy matrix. They make the FFRE laminates to be more stable when exposed to hygrothermal conditioning. Therefore, the T_g of both pure FFRE and CNFs/FFRE laminates has a slight increase after a long-term immersion.

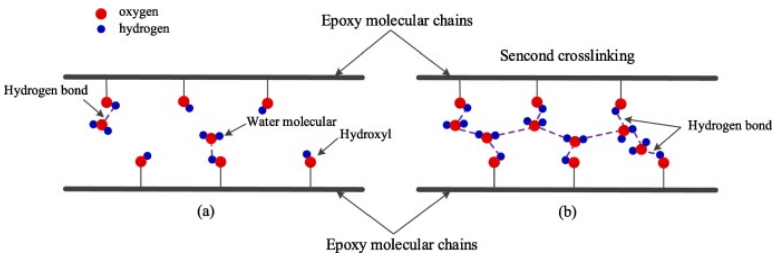

Fig. 16. Two ways of bound water combined with the epoxy matrix. (a) water molecules form one hydrogen bond with epoxy molecular chains (b) water molecules form multiple hydrogen bonds with epoxy molecular chains. (For interpretation of the references to colour in this figure legend, the reader is referred to the web version of this article.)

3.5. FTIR analysis

FTIR analysis was used to characterize the changes in bands and functional groups of pure FFRE and CNFs/FFRE laminates exposed to the hygrothermal ageing environment. Fig. 17 presents the FTIR spectrums of the unaged and aged samples from the range of 4000 cm^{-1} to 650 cm^{-1}. It can be seen from Fig. 17a that there was no new characteristic peak appeared after incorporating CNFs, which means that the chemical structure of the CNFs/FFRE was not changed. For the relative bands and functional groups of the epoxy matrix, the characteristic peak between 3600 cm^{-1} and 3000 cm^{-1} corresponded to the stretching of hydroxyl (-OH) groups. The stretching vibration of methyl ($-CH_3$) and methylene groups ($-CH_2$) were at about 2962 cm^{-1} and 2924 cm^{-1}, respectively. The bands and functional groups related to the flax fibers can be found from the characteristic peaks with wavenumbers below 2000 cm^{-1}. For example, the characteristic peaks at 1725 cm^{-1} were associated with the carbonyl (C=O) stretching, and peaks at 1605 cm^{-1} referred to the non-esterified pectin [20]. Some characteristic peaks were at 1360 cm^{-1} for the swing of $-CH_3$ and 1100 cm^{-1} for the ring stretch of symmetric glycosidic (C-O-C) [20], [55]. The stretching vibration of C-OH for the cellulose backbone was at 1080 cm^{-1} and the characteristic peak at about 1035 cm^{-1} referred to the primary alcohol of (C-O) polysaccharides [20].

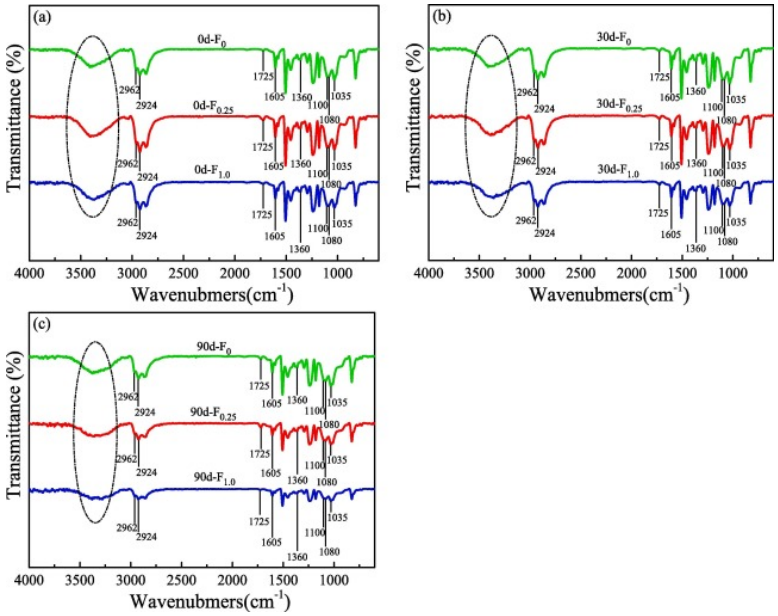

Fig. 17. FTIR spectra of unaged and aged pure FFRE and CNFs/FFRE laminates for (a) 0 days, (b) 30 days and (c) 90 days. (For interpretation of the references to colour in this figure legend, the reader is referred to the web version of this article.)

Fig. 17b and c present the changes in transmittance of some characteristic bands and functional groups after ageing compared with Fig. 17a. For the epoxy matrix, the transmittance of the aforementioned characteristic peaks (3600 cm^{-1} to 3000 cm^{-1}, 2962 cm^{-1}, and 2924 cm^{-1}) increased as the increase of ageing time. This means the number of these bands and functional groups decreased due to the severe hydrolysis reaction of the epoxy matrix. The macromolecular polymer segments were broken down into small molecular segments, which caused the epoxy matrix to be dissolved. This confirmed that some defects developed in the epoxy matrix due to the ageing, which were also observed by SEM images. Additionally, it can be seen in Fig. 17b and c that the transmittance of –OH of pure FFRE laminates between 3600 cm^{-1} and 3000 cm^{-1} was lower than that of CNFs/FFRE laminates after ageing. This change of –OH indicated that pure FFRE laminates absorbed more water than CNFs/FFRE laminates during hygrothermal ageing, which is consistent with the water uptake results. For the change of flax fiber after ageing, the transmittance of characteristic bands and functional groups below 2000 cm^{-1} of pure FFRE laminates were lower than that of CNFs/FFRE laminates after 90-days ageing as shown in Fig. 17c, which indicates more relative bands and functional groups of flax fiber existed in aged FFRE samples than those in aged CNFs/FFRE samples. Therefore, it can be inferred that the rate of hydrolysis of flax fiber in pure FFRE laminates was faster than that in CNFs/FFRE laminates.

The ageing mechanism of pure FFRE and CNFs/FFRE laminates can be illustrated in Fig. 18 according to the changes of bands and functional groups exhibited by FTIR spectrum. At the beginning of ageing, it can be seen from Fig. 18a that the epoxy matrix and flax fiber were intact for both pure FFRE and CNFs/FFRE laminates. When the pure FFRE and CNFs/FFRE laminates were immersed in distilled water, the ageing process of samples firstly began with the degradation of the epoxy matrix due to the hydrolysis reaction, leading to the generation of some micro-cracks. Afterward, the flax fiber absorbed water, which entered through the micro-cracks of the epoxy matrix, and began to hydrolyze. The structure and components of flax fiber are shown in Fig. 18. In the early stage of ageing, the

hemicellulose and pectin of flax fiber in pure FFRE laminates were firstly dissociated from the fiber because of their low molecular weight [20], at which time the hemicellulose and pectin of flax fiber in CNFs/FFRE laminates had not been completely hydrolyzed due to the relatively small amount of water uptake. Since the cellulose accounted for a large proportion of the components of the flax fibers, the change of relative bands and functional groups of pure FFRE and CNFs/FFRE laminates in the FTIR spectrum (Fig. 17b) was not significant although some pectin and hemicellulose had been dissociated at this time. With the increase of ageing degree, the high molecular weight celluloses of the flax fibers began to hydrolyze due to a lot of ether bonds (C-O-C) of the cellulose backbone broken down as shown in Fig. 18b. Some low molecular chains hydrolyzed from the celluloses were formed, such as polysaccharides and monosaccharides. Although the flax fiber in pure FFRE laminates and CNFs/FFRE laminates had been aged, the ageing degree of the celluloses in CNFs/FFRE laminates was milder than that of pure FFRE laminates because the ageing rate of CNFs/FFRE laminates was slower than that of pure FFRE laminates. These polysaccharides and monosaccharides, which were hydrolyzed from hemicelluloses and celluloses, had similar bands and functional groups [56]. This caused that the numbers of relative bands and functional groups of pure FFRE laminates were more than that of CNFs/FFRE laminates. Therefore, the transmittance of relative bands and groups of flax fiber in pure FFRE laminates exhibited in the FTIR spectrums was lower than that in CNFs/FFRE laminates, which means that the hydrolysis of pure FFRE laminates was severer than that of CNFs/FFRE laminates.

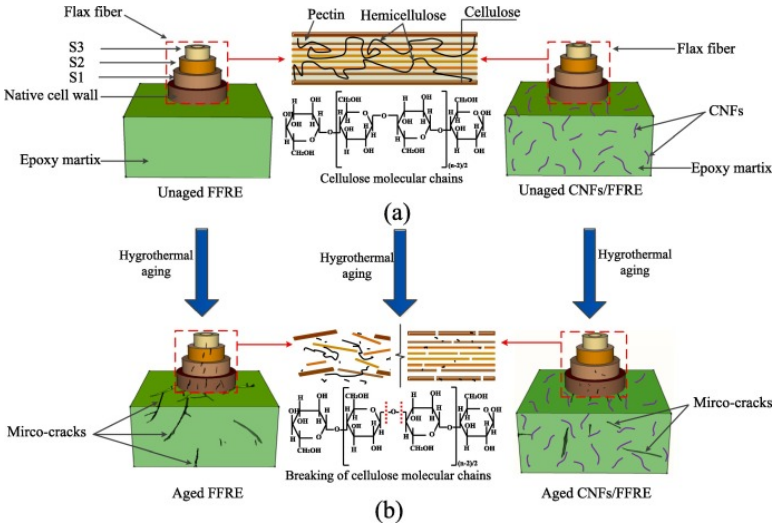

Fig. 18. The ageing mechanism of pure FFRE and CNFs/FFRE laminates under hygrothermal conditions. (a) unaged pure FFRE and CNFs/FFRE laminates and (b) aged pure FFRE and CNFs/FFRE laminates. (For interpretation of the references to colour in this figure legend, the reader is referred to the web version of this article.)

Combined with the other test results in this study, it can be concluded that the presence of CNFs slowed down the ageing process of CNFs/FFRE laminates effectively by strengthening the epoxy matrix and the interface adhesion. Additionally, it can also be found in Fig. 17b that the transmittance of relative bands and groups of flax fiber in $F_{1.0}$ after 90-days ageing was higher than that in $F_{0.25}$, which indicates that the CNFs with amount of 1.0 wt% in the epoxy matrix showed the best effect on slowing down the ageing of FFRE laminates in this study.

4. Conclusions

In this study, the hygrothermal ageing behavior of FFRE laminates after adding CNFs subjected to distilled water was experimentally investigated, and the ageing mechanism of CNFs/FFRE laminates was also studied. From this study, following conclusions can be drawn:

(1) The addition of CNFs had a positive effect on improving the hygrothermal ageing behavior of FFRE laminates. The CNFs/FFRE laminates containing 1.0 wt% CNFs showed best hygrothermal ageing behavior among the laminates with 0.25 wt% to 2.0 wt% of CNFs tested in this study.

(2) As the CNFs amount was increased from 0 to 2.0 wt%, the water uptake of CNFs/FFRE laminates first declined till 1.0 wt% CNFs, and then increased when the amount of CNFs increased to 2.0 wt%, but was still lower than that of pure FFRE laminates. It is because that hydrophobic CNFs not only occupied some voids in the matrix, but also created a tortuous diffusion path to delay the water molecules' movement in the FFRE laminates.

(3) The tensile strength and tensile elastic modulus of CNFs/FFRE laminates under hygrothermal conditioning were enhanced as the amount of CNFs increased to 1.0 wt%. This is because that the adding of CNFs not only improved the stability of the epoxy matrix, but also strengthened the interface bonding between the flax fibers and the epoxy matrix, which were observed on the SEM images of the fractured surfaces of the specimens.

(4) The storage modulus of CNFs/FFRE laminates was improved compared with that of pure FFRE laminates before and after hygrothermal ageing. This is because that CNFs made steric hindrance inside the epoxy matrix of FFRE laminates and increased the cross-linking density of the epoxy matrix. The glass transition temperature (T_g) of both CNFs/FFRE and pure FFRE increased slightly after immersed in distilled water because the bound water of Type II formed multiple hydrogen bonds with epoxy molecular chains.

(5) The changes of relative bands and functional groups presented in the FTIR spectrums indicated that the ageing rate of CNFs/FFRE laminates exposed to the hygrothermal environment was slower than that of pure FFRE laminates. This is because that CNFs strengthened the epoxy matrix and restricted the water diffusion in the laminates. The amount of 1.0 wt% CNFs showed best effect on slowing down the ageing of the FFRE laminates in this study. Therefore, adding appropriate amount of CNFs into FFRE laminates is beneficial to improve the long-term hygrothermal durability of FFRE laminates.

CRediT authorship contribution statement

Yanlei Wang: Conceptualization, Supervision, Funding acquisition, Writing - review & editing. **Wanxin Zhu:** Investigation, Writing - original draft, Data curation, Formal analysis. **Baolin Wan:** Supervision, Investigation, Writing - review & editing. **Ziping Meng:** Methodology, Investigation. **Baoguo Han:** Supervision, Methodology, Writing - review & editing.

Declaration of Competing Interest

The authors declare that they have no known competing financial interests or personal relationships that could have appeared to influence the work reported in this paper.

Acknowledgements

The authors are grateful for the financial support from the National Key Research and Development Program of China (Project No. 2017YFC0703000), the National Natural Science Foundation of China (Project Nos. 51778102 and 51978126), and the Natural Science Foundation of Liaoning Province of China (Project No. 20180550763).

Data availability

The raw and processed data required to reproduce these results are available by contacting the authors.

References

[1] Q. Han, W. Yuan, Y. Bai, X. Du. **Compressive behavior of large rupture strain (LRS) FRP-confined square concrete columns: experimental study and model evaluation.** Mater Struct, 53 (4) (2020), p. 99

[2] Y. Wang, G. Cai, A. Si Larbi, D. Waldmann, K.D. Tsavdaridis, J. Ran. **Monotonic axial compressive behaviour and confinement mechanism of square CFRP-steel tube confined concrete.** Eng Struct, 217 (2020), p. 110802

[3] Y.L. Bai, Z.W. Yan, T. Ozbakkaloglu, Q. Han, J.G. Dai, D.J. Zhu. **Quasi-static and dynamic tensile properties of large-rupture-strain (LRS) polyethylene terephthalate fiber bundle.** Constr Build Mater, 232 (2020), p. 117241

[4] Y. Wang, G. Chen, B. Wan, G. Cai, Y. Zhang. **Behavior of circular ice-filled self-luminous FRP tubular stub columns under axial compression.** Constr Build Mater, 232 (2020), p. 117287

[5] Y. Wang, G. Cai, Y. Li, D. Waldmann, A. Si Larbi, K.D. Tsavdaridis. **Behavior of circular fiber-reinforced polymer-steel-confined concrete columns subjected to reversed cyclic loads: experimental studies and finite-element analysis.** J Struct Eng, 145 (9) (2019), p. 04019085

[6] Y.L. Bai, J.G. Dai, M. Mohammadi, G. Lin, S.J. Mei. **Stiffness-based design-oriented compressive stress-strain model for large-rupture-strain (LRS) FRP-confined concrete.** Compos Struct, 223 (2019), p. 110953

[7] Y. Zhang, Y. Wei, J. Bai, G. Wu, Z. Dong. **A novel seawater and sea sand concrete filled FRP-carbon steel composite tube column: concept and behaviour.** Compos Struct, 246 (2020), p. 112421

[8] Y. Wei, Y. Zhang, J. Chai, G. Wu, Z. Dong. **Experimental investigation of rectangular concrete-filled fiber reinforced polymer (FRP)-steel composite tube columns for various corner radii.** Compos Struct, 244 (2020), p. 112311

[9] J. Li, J. Xie, F. Liu, Z. Lu. **A critical review and assessment for FRP-concrete bond systems with epoxy resin exposed to chloride environments.** Compos Struct, 229 (2019), p. 111372

[10] Q. Cao, X. Li, J. Zhou, Z.J. Ma. **Expansive concrete confined by CFRP under eccentric compression.** Constr Build Mater, 208 (2019), pp. 113-124

[11] S. Ghasemi, M. Tajvidi, D. Bousfield, D. Gardner. **Reinforcement of natural fiber yarns by cellulose nanomaterials: a multi-scale study.** Ind Crops Prod, 111 (2018), pp. 471-481

[12] V. Fiore, T. Scalici, D. Badagliacco, D. Enea, G. Alaimo, A. Valenza. **Aging resistance of bio-epoxy jute-basalt hybrid composites as novel multilayer structures for cladding.** Compos Struct, 160 (2017), pp. 1319-1328
[13] C. Wang, S. Liu, Z. Ye. **Mechanical, hygrothermal ageing and moisture absorption properties of bamboo fibers reinforced with polypropylene composites.** J Reinf Plast Compos, 35 (13) (2016), pp. 1062-1074
[14] K. Senthilkumar, N. Saba, N. Rajini, M. Chandrasekar, M. Jawaid, S. Siengchin, *et al.* **Mechanical properties evaluation of sisal fibre reinforced polymer composites: a review.** Constr Build Mater, 174 (2018), pp. 713-729
[15] G. Ma, L. Yan, W. Shen, D. Zhu, L. Huang, B. Kasal. **Effects of water, alkali solution and temperature ageing on water absorption, morphology and mechanical properties of natural FRP composites: Plant-based jute vs. mineral-based basalt.** Compos Part B Eng, 153 (2018), pp. 398-412
[16] C. Baley. **Analysis of the flax fibres tensile behaviour and analysis of the tensile stiffness increase.** Compos Part A Appl Sci Manuf, 33 (7) (2002), pp. 939-948
[17] K. Charlet, C. Baley, C. Morvan, J. Jernot, M. Gomina, J. Bréard. **Characteristics of Hermès flax fibres as a function of their location in the stem and properties of the derived unidirectional composites.** Compos Part A Appl Sci Manuf, 38 (8) (2007), pp. 1912-1921
[18] A. Thuault, S. Eve, D. Blond, J. Bréard, M. Gomina. **Effects of the hygrothermal environment on the mechanical properties of flax fibres.** J Compos Mater, 48 (14) (2014), pp. 1699-1707
[19] Y. Wang, G. Chen, B. Wan, B. Han. **Compressive behavior of circular sawdust-reinforced ice-filled flax FRP tubular stub columns.** Materials (Basel), 13 (4) (2020), p. 957
[20] Y. Li, B. Xue. **Hydrothermal ageing mechanisms of unidirectional flax fabric reinforced epoxy composites.** Polym Degrad Stab, 126 (2016), pp. 144-158
[21] A. Gomes, T. Matsuo, K. Goda, J. Ohgi. **Development and effect of alkali treatment on tensile properties of curaua fiber green composites.** Compos Part A Appl Sci Manuf, 38 (8) (2007), pp. 1811-1820
[22] S. Basu, U. Shivhare, S. Muley. **Moisture adsorption isotherms and glass transition temperature of pectin.** J Food Sci Technol, 50 (3) (2013), pp. 585-589
[23] S. Ouajai, R. Shanks. **Composition, structure and thermal degradation of hemp cellulose after chemical treatments.** Polym Degrad Stab, 89 (2) (2005), pp. 327-335
[24] T. Doan, S. Gao, E. Mäder. **Jute/polypropylene composites I. Effect of matrix modification.** Compos Sci Technol, 66 (7–8) (2006), pp. 952-963
[25] A. Edeerozey, H. Akil, A. Azhar, M. Ariffin. **Chemical modification of kenaf fibers.** Mater Lett, 61 (10) (2007), pp. 2023-2025
[26] A. Retegi, A. Arbelaiz, P. Alvarez, R. Llano-Ponte, J. Labidi, I. Mondragon. **Effects of hygrothermal ageing on mechanical properties of flax pulps and their polypropylene matrix composites.** J Appl Polym Sci, 102 (4) (2006), pp. 3438-3445
[27] S. Joshi, L. Drzal, A. Mohanty, S. Arora. **Are natural fiber composites environmentally superior to glass fiber reinforced composites?** Compos Part A Appl Sci Manuf, 35 (3) (2004), pp. 371-376
[28] J. Cha, J. Kim, S. Ryu, S. Hong. **Comparison to mechanical properties of epoxy nanocomposites reinforced by functionalized carbon nanotubes and graphene nanoplatelets.** Compos Part B Eng, 162 (2019), pp. 283-288
[29] Z. Pi, H. Xiao, J. Du, M. Liu, H. Li. **Interfacial microstructure and bond strength of nano-SiO_2-coated steel fibers in cement matrix.** Cem Concr Compos, 103 (2019), pp. 1-10

[30] C. García, M. Fittipaldi, L. Grace. **Epoxy/montmorillonite nanocomposites for improving aircraft radome longevity.** J Appl Polym Sci, 132 (43) (2015), pp. 1-9
[31] M. Demirci, N. Tarakçıoğlu, A. Avcı, A. Akdemir, İ. Demirci. **Fracture toughness (Mode I) characterization of SiO_2 nanoparticle filled basalt/epoxy filament wound composite ring with split-disk test method.** Compos Part B Eng, 119 (2017), pp. 114-124
[32] M. Lu, H. Xiao, M. Liu, X. Li, H. Li, L. Sun. **Improved interfacial strength of SiO_2 coated carbon fiber in cement matrix.** Cem Concr Compos, 91 (2018), pp. 21-28
[33] T. Ozkan, M. Naraghi, I. Chasiotis. **Mechanical properties of vapor grown carbon nanofibers.** Carbon, 48 (1) (2010), pp. 239-244
[34] Y. Wang, Y. Wang, B. Wan, B. Han, G. Cai, Z. Li. **Properties and mechanisms of self-sensing carbon nanofibers/epoxy composites for structural health monitoring.** Compos Struct, 200 (2018), pp. 669-678
[35] Y. Wang, Y. Wang, B. Han, B. Wan, G. Cai, R. Chang. **In situ strain and damage monitoring of GFRP laminates incorporating carbon nanofibers under tension.** Polymers (Basel), 10 (7) (2018), p. 777
[36] L. Zhang, J. Ma. **Effect of carbon nanofiber reinforcement on mechanical properties of syntactic foam.** Mater Sci Eng A, 574 (2013), pp. 191-196
[37] Y. Wang, Y. Wang, B. Han, B. Wan, G. Cai, Z. Li. **Strain monitoring of concrete components using embedded carbon nanofibers/epoxy sensors.** Constr Build Mater, 186 (2018), pp. 367-378
[38] S. Saha, S. Bal. **Long term hydrothermal effect on the mechanical and thermo-mechanical properties of carbon nanofiber doped epoxy composites.** J Polym Eng, 38 (3) (2018), pp. 251-261
[39] G. Jefferson, B. Farah, M. Hempowicz, K. Hsiao. **Influence of hygrothermal aging on carbon nanofiber enhanced polyester material systems.** Compos Part B Eng, 78 (2015), pp. 319-323
[40] R. Kattaguri, A. Fulmali, R. Prusty, B. Ray. **Effects of acid, alkaline, and seawater aging on the mechanical and thermomechanical properties of glass fiber/epoxy composites filled with carbon nanofibers.** J Appl Polym Sci, 137 (10) (2019), p. 48434
[41] ASTM D570-10. Standard test method for water absorption of plastics. West Conshohocken, PA: ASTM International; 2010.
[42] ASTM D3039/D3039M-14. Standard test method for tensile properties of polymer matrix composite materials. West Conshohocken, PA: ASTM International; 2014.
[43] ASTM D4065/D4065-12. Standard Practice for Plastics: Dynamic Mechanical Properties: Determination and Report of Procedures. West Conshohocken, PA: ASTM International; 2012.
[44] L. Bao, A. Yee, C. Lee. **Moisture absorption and hygrothermal aging in a bismaleimide resin.** Polymer, 42 (17) (2001), pp. 7327-7333
[45] P. Jojibabu, G. Ram, A. Deshpande, S. Bakshi. **Effect of carbon nano-filler addition on the degradation of epoxy adhesive joints subjected to hygrothermal aging.** Polym Degrad Stab, 140 (2017), pp. 84-94
[46] J. Zhou, J. Lucas. **Hygrothermal effects of epoxy resin. Part I: The nature of water in epoxy.** Polymer, 40 (20) (1999), pp. 5505-5512
[47] Y. Wang, Y. Wang, B. Wan, B. Han, G. Cai, R. Chang. **Strain and damage self-sensing of basalt fiber reinforced polymer laminates fabricated with carbon nanofibers/epoxy composites under tension.** Compos Part A Appl Sci Manuf, 113 (2018), pp. 40-52
[48] J. Park, Z. Wang, J. Jang, J. Gnidakoung, W. Lee, J. Park, *et al.* **Interfacial and hydrophobic evaluation of glass fiber/CNT-epoxy nanocomposites using electro-micromechanical technique and wettability test.** Compos Part A Appl Sci Manuf, 40 (2009), pp. 1722-1731

[49] M. Ahmadi, M. Masoomi, S. Safi, O. Zabihi. **Interfacial evaluation of epoxy/carbon nanofiber nanocomposite reinforced with glycidyl methacrylate treated UHMWPE fiber.** J Appl Polym Sci, 133 (2016), pp. 1-11

[50] M. Mohammadalipour, M. Masoomi, M. Ahmadi, S. Safi. **Interfacial shear strength characterization of GMA-grafted UHMWPE fiber/epoxy/nano clay hybrid nanocomposite materials.** RSC Adv, 6 (2016), pp. 41793-41799

[51] G. Wu, L. Ma, Y. Wang, L. Liu, Y. Huang. **Improvements in interfacial and heat-resistant properties of carbon fiber/methylphenylsilicone resins composites by incorporating silica-coated multi-walled carbon nanotubes.** J Adhes Sci Technol, 30 (2016), pp. 117-130

[52] X. Shen, J. Jia, C. Chen, Y. Li, J. Kim. **Enhancement of mechanical properties of natural fiber composites via carbon nanotube addition.** J Mater Sci, 49 (2014), pp. 3225-3233

[53] G. Gkikas, D. Douka, N. Barkoula, A. Paipetis. **Nano-enhanced composite materials under thermal shock and environmental degradation: a durability study.** Compos Part B Eng, 70 (2015), pp. 206-214

[54] Q. Cao, H. Li, Z. Lin. **Effect of active confinement on GFRP confined expansive concrete under axial cyclic loading.** ACI Struct. J., 117 (1) (2020), pp. 207-216

[55] S. Lin, J. Zhang, J. Yuan, Y. Yuan, J. Shen. **Chemical modification of cellulose membranes with sulfo ammonium zwitterionic vinyl monomer to improve hemocompatibility.** Colloids Surf. B Biointerfaces, 30 (3) (2003), pp. 249-257

[56] S. Alix, E. Philippe, A. Bessadok, L. Lebrun, C. Morvan, S. Marais. **Effect of chemical treatments on water sorption and mechanical properties of flax fibres.** Bioresour. Technol., 100 (20) (2009), pp. 4742-4749